Coastal Environmental and Ecosystem Issues of the East China Sea,
Eds., A. Ishimatsu and H.-J. Lie, pp. 49–70.

Enhanced Movements of Sands off the Saemangeum Dyke by an Interplay of Dyke Construction and Winter Monsoon

Hee Jun LEE

Marine Geology Laboratory, Korea Ocean Research & Development Institute, Ansan, P.O. Box 29, Seoul 425-600, Korea

Abstract—The sandy nearshore areas off sectors I and II of the Saemangeum Dyke were investigated to unravel the effects of the dyke and winter monsoon on the sand movements accelerated southward during 2003–2006. The sands had covered rapidly much of the otherwise muddy seabed during only 3 years, an unusual phenomenon in natural environments on the western coastal region of Korea. Although current measurements with a benthic tripod (TISDOS) show a residual current flowing southward, these alone could hardly transport the seabed sands. During winter, northerly or northwesterly winds should induce wind-generated currents that add hydrodynamic energy strong enough to move sands as bedload to the tidal currents. The areal increase in gravel occurrences within the original sand deposit suggests that the hydraulically equivalent sand grains were selectively transported south with coarser materials left behind. The dyke emplacement is inferred to modify tidal regime to create southward flowing residual currents. However, the sand transport may have been virtually hindered with remarkably weakened tidal currents since the closing of the opening gaps in April 2006. In summary, the combination of the dyke and winter monsoon resulted in a fast expansion of seabed sands, an extraordinary process rarely found in the natural nearshore environments far from any estuary.

Keywords: sediment transport, surface sediment, bathymetry, macrotidal, monsoon, winter wave, Saemangeum Dyke, Yellow Sea

1. INTRODUCTION

The eastern Yellow Sea is subjected to a prominent monsoonal seasonality in the meso-to-macro tidal regime. The Asian monsoon system is characterized by meteorological conditions of mild summertime and harsh wintertime prevailing over the Asian continent-bound seas, South China and East China as well as Yellow (Webster et al., 1998; Clemens et al., 2003). Tidal currents are frequently strong enough to move seafloor sands and resuspend muddy sediments from the shallow water depths of nearshore and tidal flats, particularly during spring tide (Lee et al., 2004, 2005). Sand movements have been comprehensively documented on tidal flats in a semi-enclosed bay (Garolim Bay) from a hydrodynamic viewpoint, which shows that the medium-scale (2 m wavelength and 0.7 m height) sand waves could move only during spring tide (Lee et al., 2004). In deeper nearshore, a train of sand waves

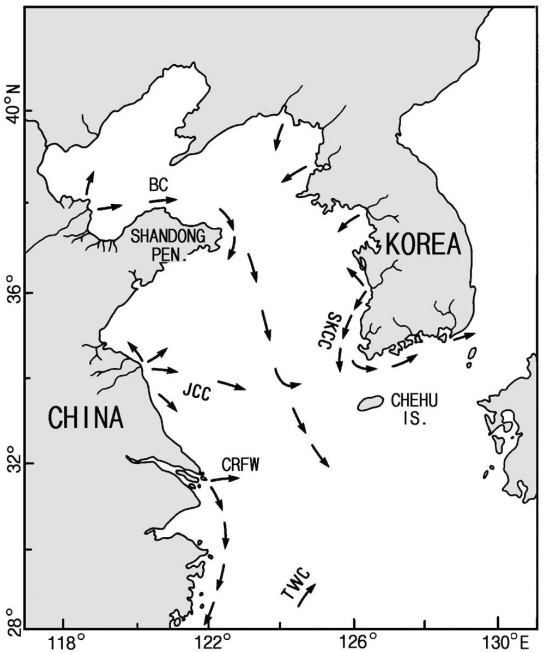

Fig. 1. Schematic of suspended sediments dispersal in the Yellow Sea. Reprinted from *Marine Geology*, **87**, Lee and Chough, Sediment distribution, dispersal and budget in the Yellow Sea, 195–205, © 1989, with permission from Elsevier.

mostly found on the back of large tidal sand ridges or banks indicate that the sands on a large bedform are mobile by spring tidal currents and/or combined tidal currents and waves (Lee et al., 2005). During winter, high waves and wind-generated currents consistently make the sediment transport by tidal currents more effective and easier even in the bottom boundary layer of considerably deep (possibly more than 20 m) waters (Lee and Chu, 2001; Lee and Ryu, 2007). The fact that the transport of suspended sediments takes place along the western coastal areas of Korea more vigorously during winter than summer has been well established from the *in-situ* observations and satellite image analyses (Lee and Chu, 2001; Chough et al., 2004). Therefore, owing to strong tidal currents and winter monsoon, the net transport of sediments in the west coast of Korea can be generalized as being directed south all along the coast (Figs. 1 and 2) (Lee and Chough, 1989; Chough et al., 2000).

The seafloor around the Saemangeum dyke is predominantly covered with sands (Lee and Ryu, 2008). These sands have been found to be derived from the Mangyung and Dongjin rivers nearby. Before the dyke construction, the riverine sands were accumulated in the form of tidal sand ridges in and around the estuary that were aligned roughly in the NE–SW direction conforming to the major axis of the tidal currents at the time. However, the presence of the dyke has largely changed the tidal

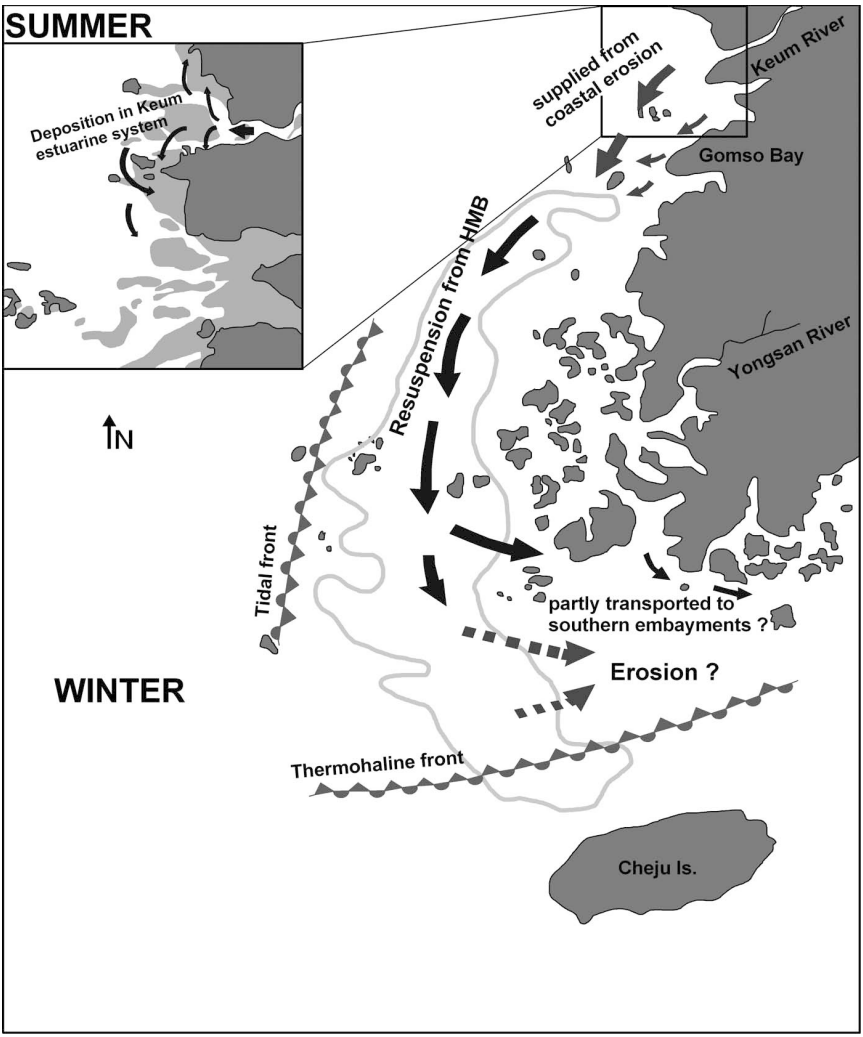

Fig. 2. Schematic of suspended sediments dispersal in the southwestern corner of Korea. Reproduced with permission of the Society for Sedimentary Geology (SEPM), from Origin of inner-shelf mud deposit in the southeastern Yellow Sea: Huksan Mud Belt, Lee and Chu, *Journal of Sedimentary Research*, **71**, 144–154, 2001, Fig. 2; permission conveyed through Copyright Clearance Center, Inc.

regime, particularly the tidal direction, aside from preventing the seafloor off the dyke from accessing sands. Such an artificial change in tidal direction resulted in the change in sediment transport conditions for the offshore surficial sands (Lee and Ryu, 2008). It seems that the construction of the dyke eventually promoted the sand movements southward in concert with winter monsoon.

The purpose of this study is to illuminate the drastic increase in the areal extent of surficial sands during the recent years, and to elucidate the causes of the sand expansion with respect to the relationships among tidal regime, winter monsoon, and the dyke construction. The results can be applied to the interpretation in terms of winter monsoon of the Holocene stratigraphy which frequently shows the upward-coarsening trend in sediment texture on the west coastal fringe of Korea.

2. STUDY AREA

The study area encompasses the nearshore off sectors I and II of the Saemangeum dyke which is bounded by the Byunsan Peninsula to the south and the Gogunsan Archipelago to the north (Fig. 3). The beach sands are thought to have originated from the Mangyung and Dongjin rivers to the north via littoral drift along the coastline before the dyke construction (KORDI, 1999). The bathymetry of the study area shows an alternating pattern of troughs and shoals roughly normal to the dyke (Fig. 4). The troughs are erosional in origin by intensified flows of tidal currents through the opening gaps, whereas the shoals have been formed with sands added from the adjacent erosional troughs (KORDI, 2006). One of the key geographical components in the study area is Byunsan Beach with well-sorted sands undergoing active wave actions directly from offshore (from NW) during winter.

The long-term (1980–2004) wind data shows that northwesterly winds occurred most frequently (30.8% occurrences) as compared with the subornate southerly winds (16.8%) (KORDI, 2005). Based on these data, the modeled values of the maximum significant height and period of waves for 20 years become highest for the waves from NW during winter, averaging 4–5 m and 9–10 s, respectively (KORDI, 2005). Tide is macrotidal with tidal ranges of 5.0 and 6.6 m at neap and spring, respectively (National Oceanographic Research Institute, 2005, 2006).

3. MATERIALS AND METHODS

Time-series measurements of hydrodynamic parameters were carried out with a sequence of benthic tripods, TISDOSs, at 3 sites off sectors I and II simultaneously for a period of 5–12 days twice, first during March and then during August 2006 (Fig. 4). The parameters measured include water depth, waves, currents, suspended sediment concentrations, temperature, salinity, and bed-level fluctuations. Currents were measured 0.1–0.7 m above the seabed (ab) with an acoustic Doppler current sensor (DCS3620, Aanderaa Instruments) as 30-second averages, and suspended sediment concentrations at 0.1 m ab with OBSs (Optical Backscatter Sensor) at 4 Hz. Two transducers (50 and 200 Hz) and a Digiquartz pressure recorded variations of seabed relief every 10 minutes and water pressure at 2 Hz, respectively. Temperature and salinity were measured simultaneously with a SBE-37 instrument of Sea-Bird at 10-minute intervals. More details of the measurements with TISDOS can be seen elsewhere (Lee et al., 2004, 2005).

Surface sediments were collected from a total of 81 sites in a regular grid over the study area and analyzed for grain size distribution in the laboratory. After calcium carbonates and organic matter were removed with 0.1 N HCl and 10% H_2O_2,

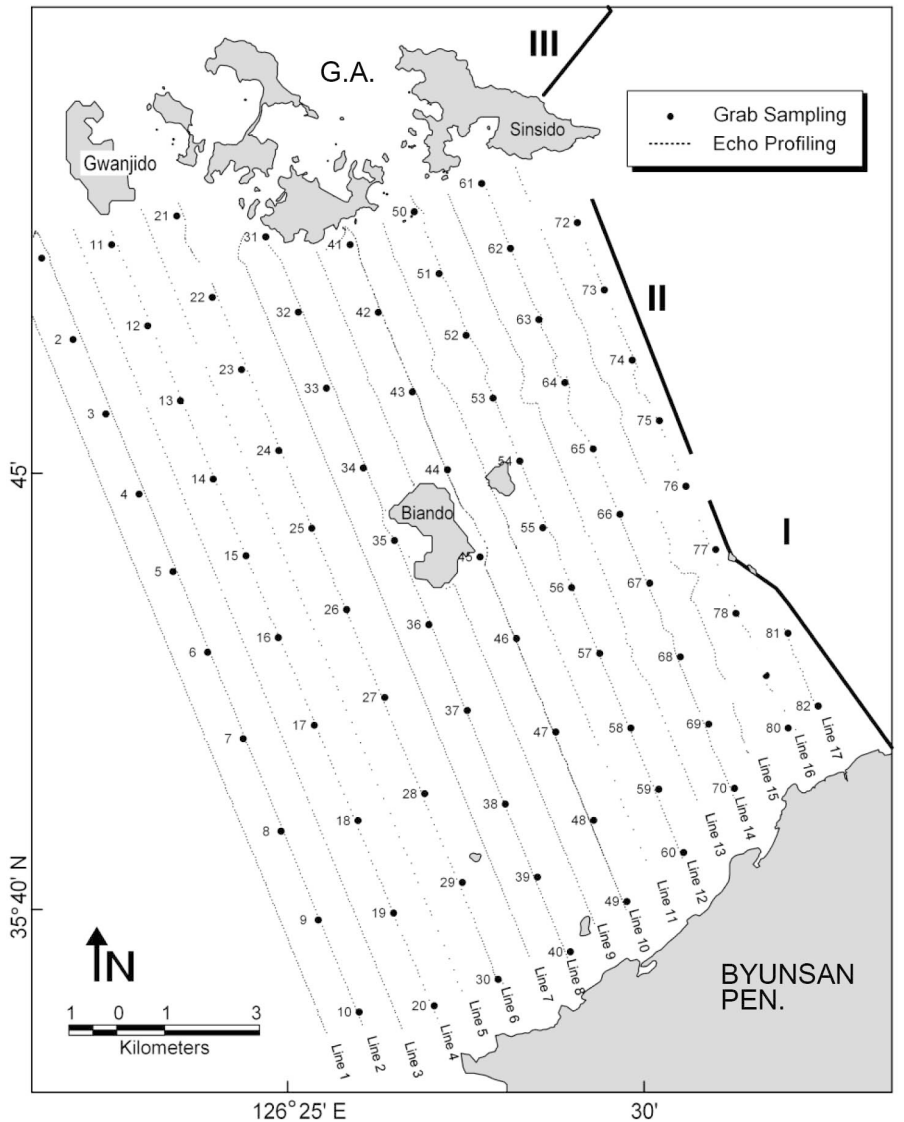

Fig. 3. Map showing study area with location of grab sampling and echo sounding before sectors I and II of the Saemangeum Dyke. G.A. stands for Gogunsan Archipelago.

respectively, each sample was separated into two particle fractions using a 4-ϕ-mech sieve. The size distributions of the fractions coarser and finer than 4 ϕ were determined by dry sieving and Sedigraph 5100, respectively.

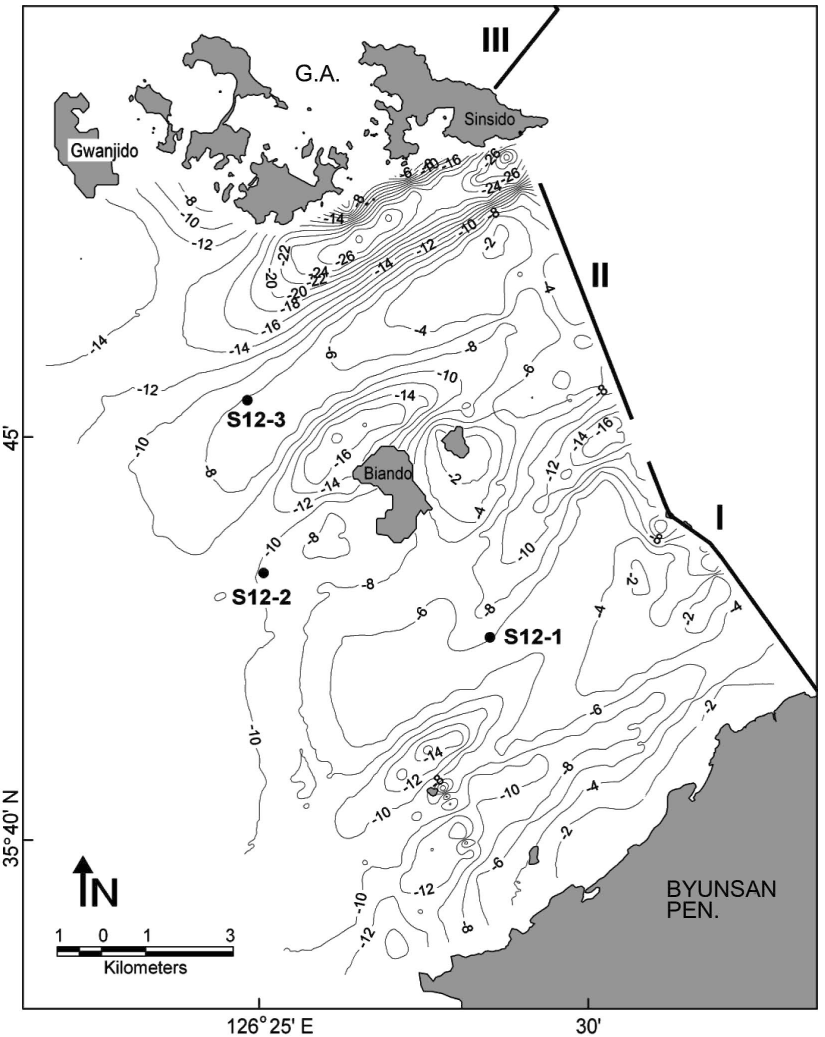

Fig. 4. Bathymetry of the seabed off sectors I and II of the dyke obtained in 2006. Contours in m relative to lowest lower water level. Dots indicate TISDOS deployment sites. G.A. stands for Gogunsan Archipelago.

4. RESULTS

4.1. Grain texture and distribution of surface sediments

The surface sediments in the study area are classified into 3 sedimentary facies, sand, muddy sand, and sandy mud (Fig. 5). Sand facies is composed exclusively of sand with trace amounts of mud (less than 5%), whereas sandy mud facies consists

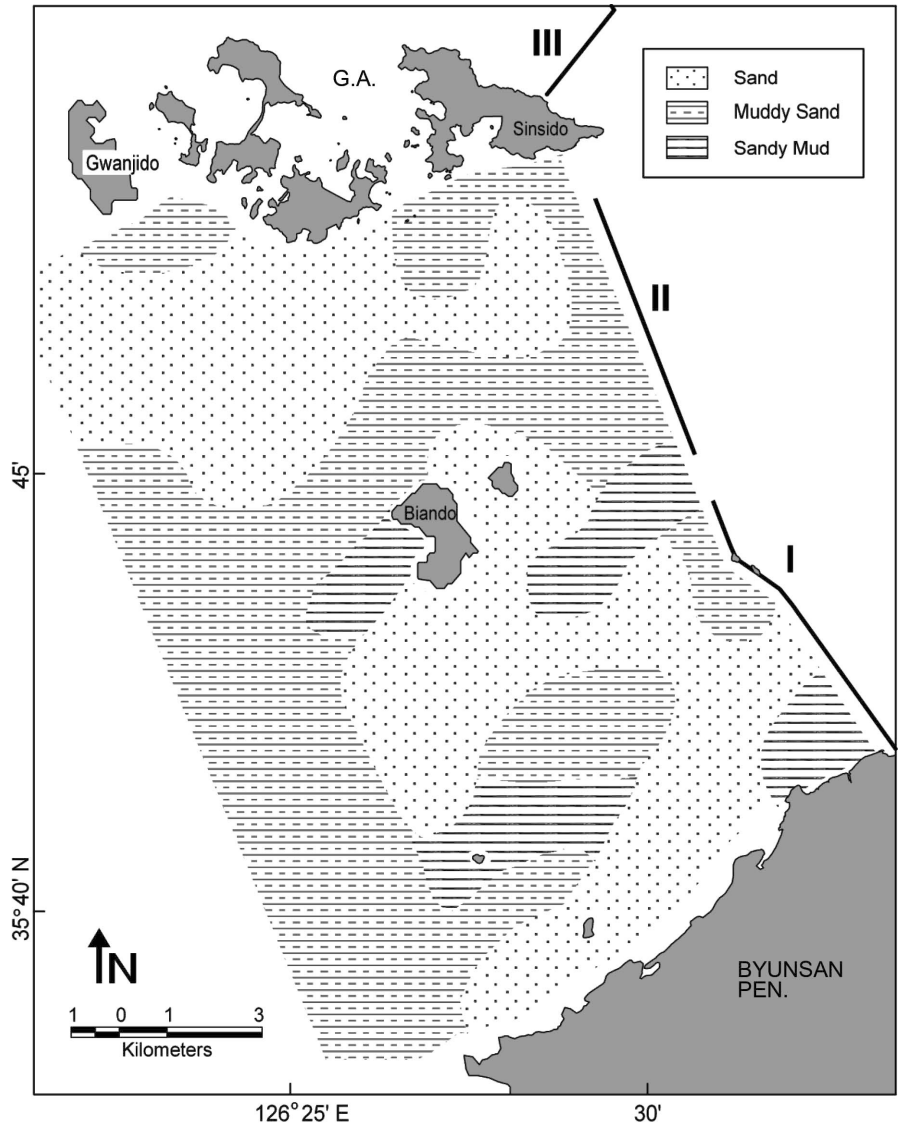

(A) 2003

Fig. 5. Distribution of surface sediments in the study area in (A) 2003 and (B) 2006.

dominantly of silt (41–76%, 53% on average) with clay (3–52%, 15% on average) and sand (4–46%, 32% on average). Muddy sand facies is considerably sandier than sandy mud facies such that the sand contents measure 77% on average in a range of 53–89%;

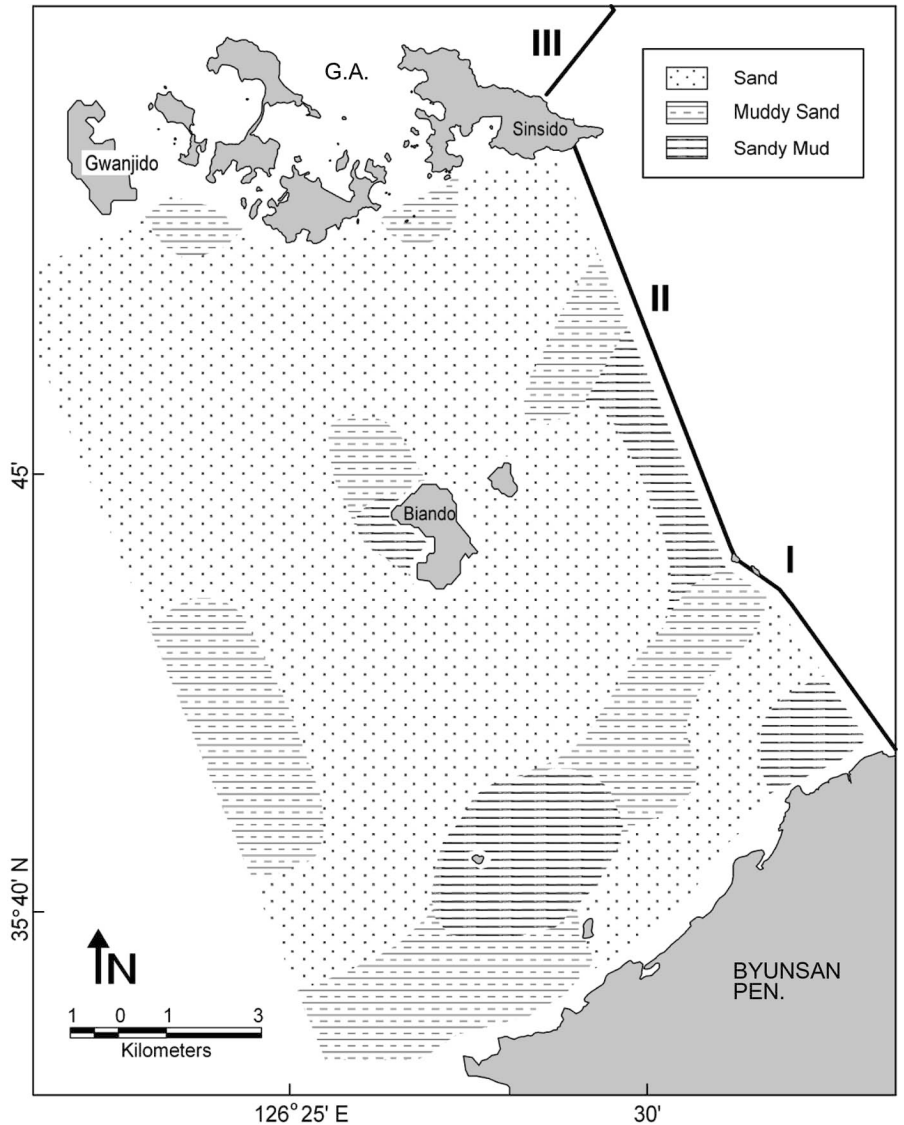

(B) 2006

Fig. 5. (continued.)

the silt and clay contents range between 11–32% (average, 19%) and 0–17% (average, 4%), respectively.

The sand facies was distributed on seabed near the Gogunsan Archipelago and Byunsan Peninsula and in the center of the surveyed area around Bian Island

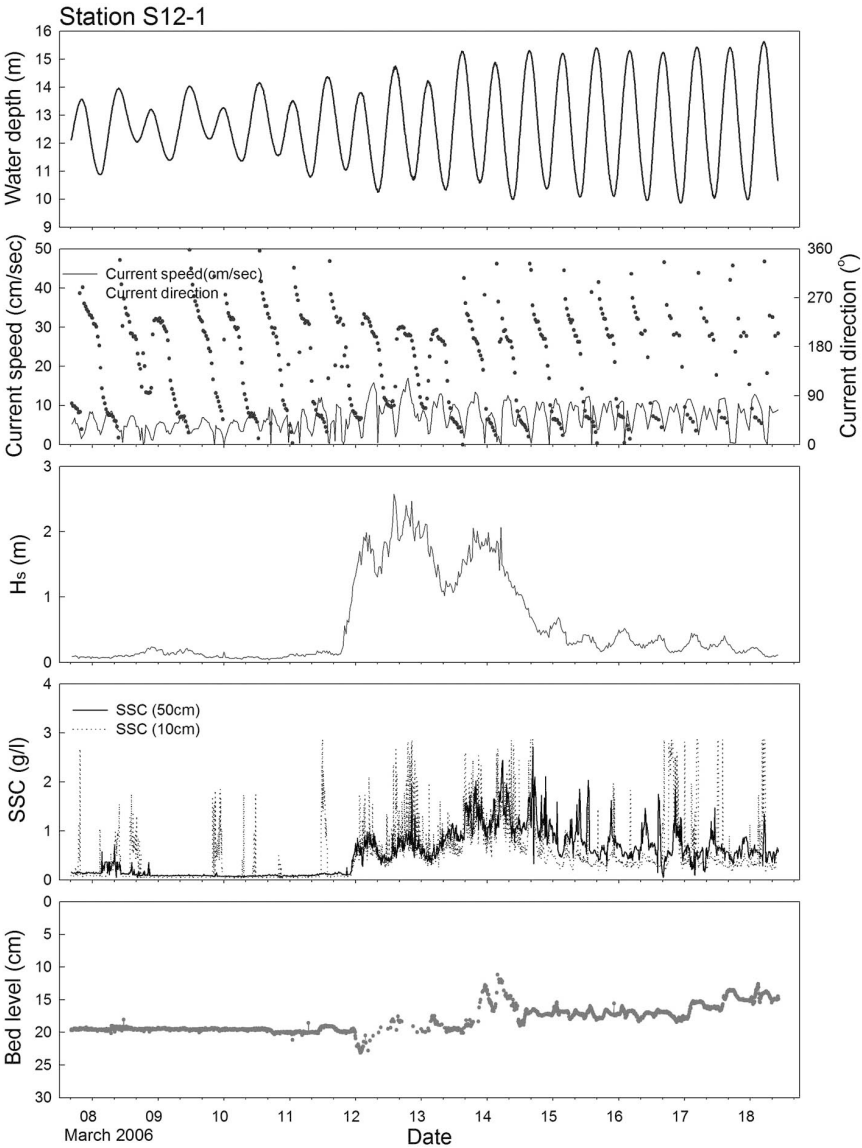

Fig. 6. Time-series of hydrodynamic measurements with TISDOS at station S12-1 in March 2006.

occupying roughly half of the surveyed area off sectors I and II in 2003 (Fig. 5a). However, the sandy area abruptly expanded to more than two thirds of the surveyed area during only 3 years from 2003 to 2006 (Fig. 5b). It is also noticeable that gravels, which initially occurred only in part of the northern sand deposit near the Gogunsan Archipelago, were now found from a more extended area.

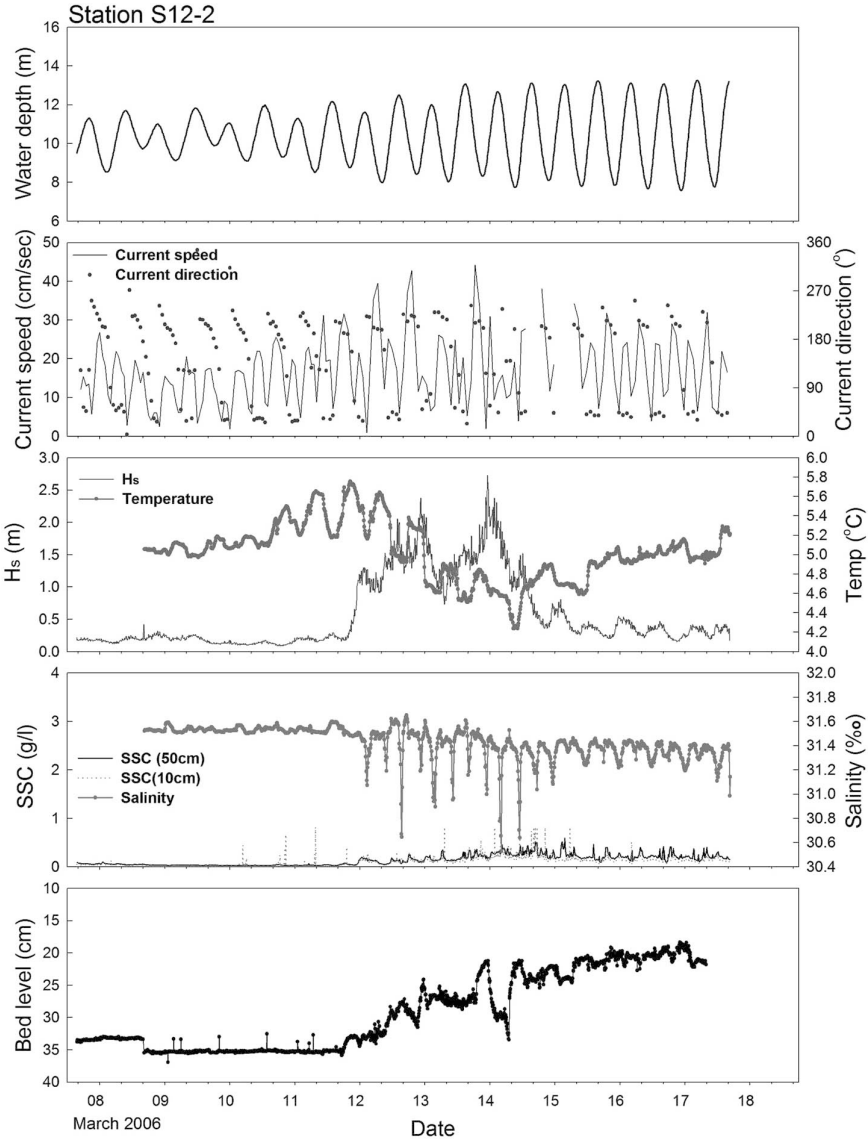

Fig. 7. Time-series of hydrodynamic measurements with TISDOS at station S12-2 in March 2006.

4.2. Hydrodynamic measurements before closing of the opening gaps (March 2006)

The tidal range measured 3 m in neap and 6 m in spring with a depth range of 7–16 m (Figs. 6–8). Diurnal inequality was largest (about 1 m) in neap, which tended to decrease gradually toward the spring.

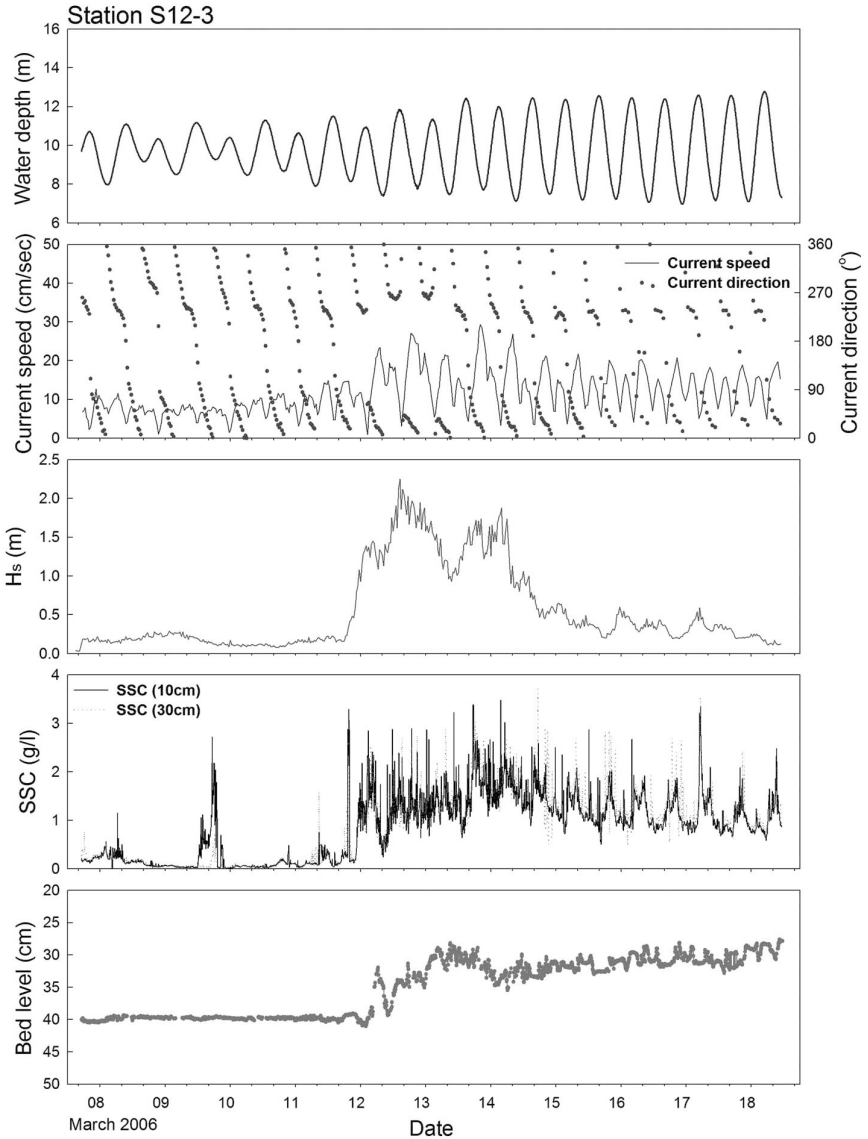

Fig. 8. Time-series of hydrodynamic measurements with TISDOS at station S12-3 in March 2006.

The current velocities 0.1 m above bed at station S12-1 increased up to 0.18 m/s during 11–14 March when waves were high with the wave height of 1.5–2.5 m, although these were generally less than 0.1 m/s in the remaining period of time when waves were nearly nonexistent (Fig. 6). Such an increase in the current

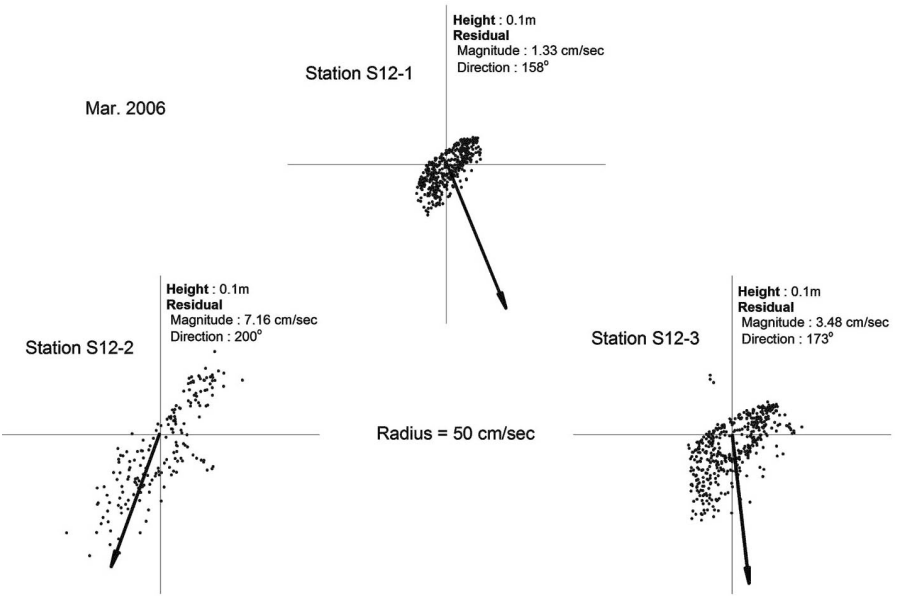

Fig. 9. Vector plot of currents with estimated residual currents from the TISDOS measurements at 3 stations off sectors I and II of the Saemangeum Dyke in March 2006. Magnitudes of residual vectors are not scaled but held constant in all the stations.

velocities can be seen from the other stations, from less than 0.3 m/s to more than 0.4 m/s and from less than 0.1 or 0.2 m/s to 0.3 m/s at stations S12-2 and S12-3, respectively (Figs. 7 and 8). The currents rotated anti-clockwise during a tidal cycle with a major tidal axis in the direction of the NE (flood)–SW (ebb). In general, ebb currents were slightly stronger than flood currents. The residual currents estimated for the whole duration of the measurements ranged between 0.01–0.07 m/s in roughly the S direction (Fig. 9).

The SSC (suspended sediment concentrations) varied basically with current velocities during transitional to spring tide, showing higher SSC at the ebb than at the flood (Figs. 6–8). Therefore, the highest SSC during a tidal cycle occurred at the peak velocities of the ebb flow. High waves during 11–14 March also played a significant role in increasing the SSC by more than 1 g/L. The SSC 0.5 m above the bed during the measurements except for the period of neap tide were in the range of 1–2, 0.3–0.5, and 1–3 g/L at stations S12-1, S12-2, and S12-3, respectively (Figs. 6–8).

At station S12-2, temperature and salinity were measured (Fig. 7). While the background temperature was about 5°C, the temperature shows a distinctive fluctuating pattern with a varying range of about 0.5°C in such a way that it rose at ebb and then fell at flood during 10–13 March. It is noticeable that the temperature shows a perceivably decreasing curve (from 5 to 4.5°C) during high waves. Salinity also shows a fluctuation pattern according to the tidal variations after 12 March: it fell at

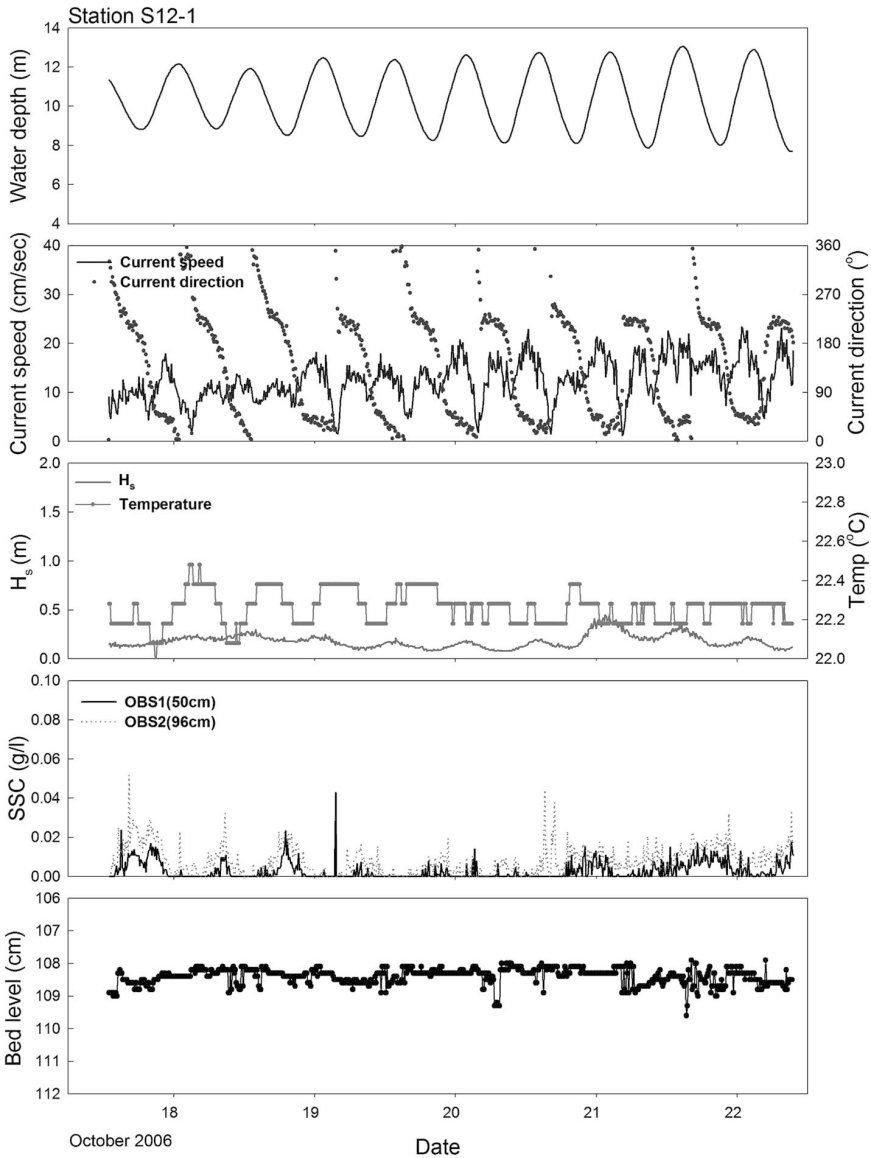

Fig. 10. Time-series of hydrodynamic measurements with TISDOS at station S12-1 in October 2006.

ebb and rose at flood in the range of 31.2–31.6‰. Since the durations of the fluctuation of temperature and salinity are not identical with one another, the reason why these fluctuations took place is unknown. Nonetheless, it might be related to the plume released from inside through the gates during the measurements.

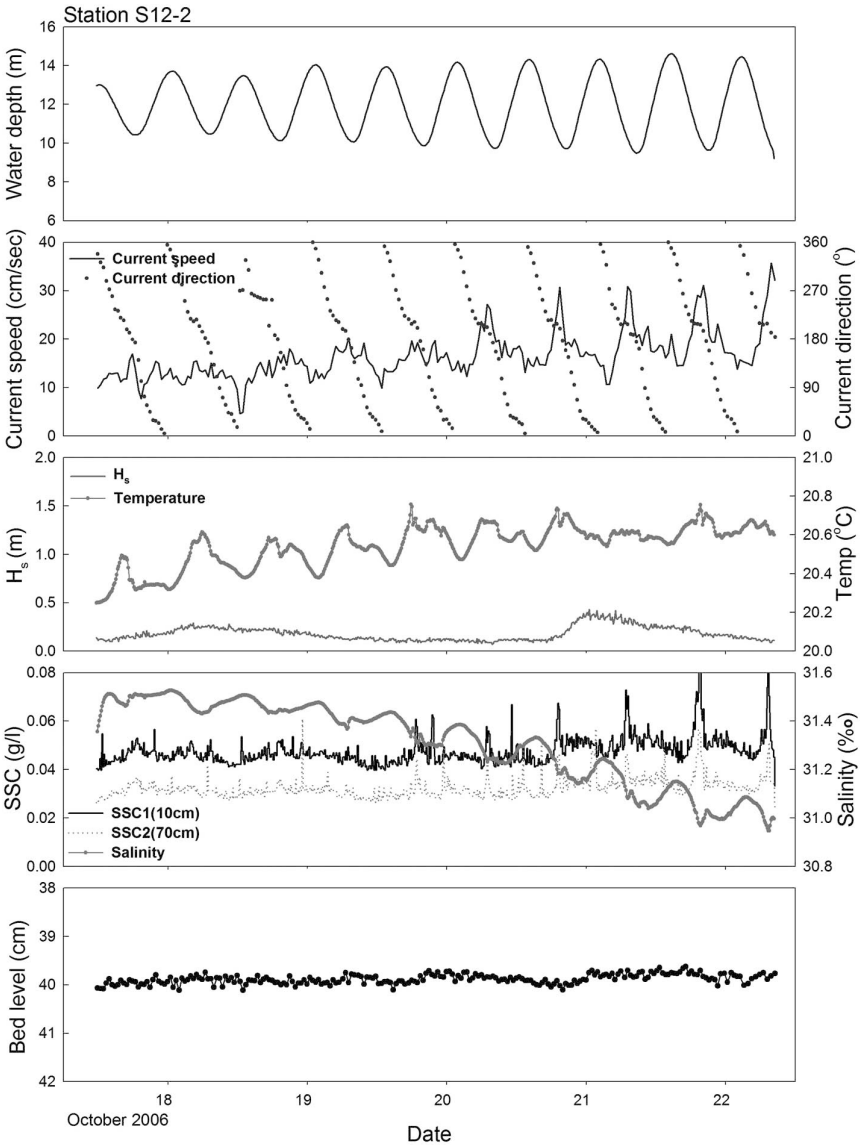

Fig. 11. Time-series of hydrodynamic measurements with TISDOS at station S12-2 in October 2006.

4.3. Hydrodynamic measurements after closing of the opening gaps (October 2006)

The tidal range measured 3–5 m during transitional and spring tide with a depth range of 7–15 m, quite similar conditions to those of March (Figs. 10–12). Diurnal inequality was less than 0.5 m in the period of the measurements lacking the neap tide.

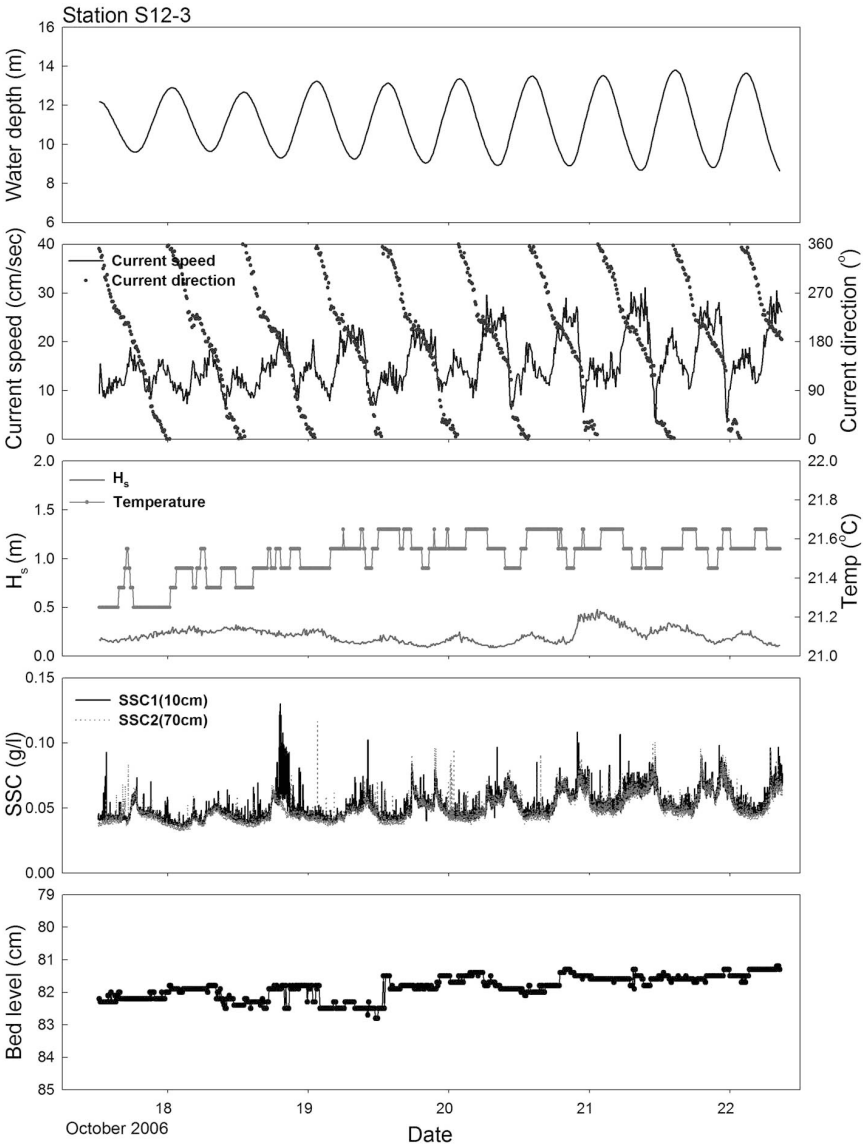

Fig. 12. Time-series of hydrodynamic measurements with TISDOS at station S12-3 in October 2006.

The currents 0.2 m above the seabed were very low (less than 0.1 m/s) with an easterly residual current velocity less than 0.01 m/s at station S12-1 (Fig. 10). For reference, the currents at 1.0 m of the seabed were still low, in the range of 0.1–0.2 m/s and show slight flood-dominance with a northwesterly residual current of

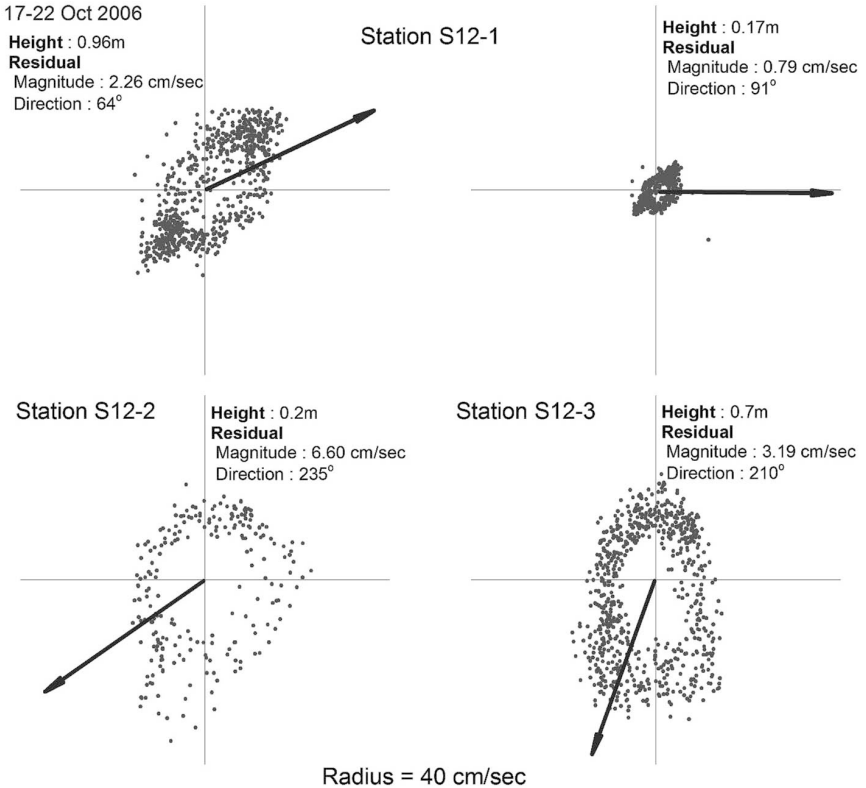

Fig. 13. Vector plot of currents with estimated residual currents from the TISDOS measurements at 3 stations off sectors I and II of the Saemangeum Dyke in October 2006. Magnitudes of residual vectors are not scaled but held constant in all the stations.

0.02 m/s (Figs. 10 and 13). At station S12-2, the ebb-dominant currents varied between 0.1 and 0.3 m/s with a southeasterly residual current of 0.07 m/s (Figs. 11 and 13). There were only current measurements at 0.7 m at station S12-3, which show a range of 0.1–0.3 m/s and a southwesterly residual of 0.03 m/s with distinctive ebb-dominance (Figs. 12 and 13). During the measurements, the fair-weather conditions (wave height less than 0.5 m) allowed no detection of wave effects on currents and suspended sediment concentrations (Figs. 10–12). In comparison to the March counterparts, the currents were generally weakened after closing of the gaps, with the current rotation during tidal cycles profoundly distinctive (Figs. 9 and 13).

The SSC were very low, largely less than 0.1 g/L at all three stations, in contrast with the March values associated with high waves commonly exceeding 1 g/L (Figs. 10–12). The relationship between currents and SSC is less distinctive than shown in the March data.

The temperature fluctuated with tidal phases in a way that it rose at ebb and fell at flood in the range of 20.3–20.7°C at station S12-2 (Fig. 11). It shows a general tendency toward a gradual increase over time. Salinity also followed a fluctuating pattern with tidal phases, similar to the temperature but with the reversing trend; it fell at ebb and rose at flood on a generally decreasing curve in a range of 31.0–31.5‰ (Fig. 11).

5. DISCUSSION AND CONCLUSIONS

The tidal regime in front of sectors I and II prior to March 2006 was still energetic by the opening gaps that allowed tidal currents to circulate across the dyke. The resulting residual currents during the measurements show a roughly southward direction, in good agreement with the southward expansion of sandy areas (Fig. 14). However, tidal currents alone could hardly drag sands as bedload without additional forcings, i.e. waves or wave-induced currents. Such a lack of competence by tidal currents alone can be seen in the non-wavy period of the March measurements as well as the whole October data in which the SSC remained very low throughout the measurements without wave influences (Figs. 10–12). The wave-induced currents most helpful in transporting sands southward may well evolve when northerly or northwesterly winds blow most frequently during winter. The combined wave-induced and tidal currents as shown by the windy duration of the March data could be now strong enough to set sands in motion, particularly during stormy days observable frequently in winter. Waves can themselves increase suspended sediment transport by resuspending bottom sediments that then move in one direction even by weak tidal currents.

The southward residual tidal current appears to be created by the dyke. In natural conditions before the onset of dyke construction, the major sand transport should have been southwestward, roughly normal to the dyke alignment, testified by the configuration of the former tidal sand ridges in an elongated form parallel with a major tidal axis lying in the NE–SW direction (KORDI, 1999). At the time, the residual current also most likely flowed in a direction other than the south, probably in a similar direction to the NE–SW major tidal axis. The sediment transport quantities by the combined current forcing (tidal and residual) are found to be greater than the simple addition of those by individual current forcings, based on simple mathematical calculations: the differences between the former and latter sediment transport quantities are proportional to uU^2, where u and U are the speeds of wave-induced currents and tidal currents, respectively, if they are practically symmetrical during tidal cycle, which is the case with the study area. It appears that the southward expansion of sandy areas has been practically ceased due to much diminished tidal currents since the closing of the open gaps in April 2006 (Fig. 14).

The hydrodynamic reinforcement by the combined effects of the dyke and winter monsoon caused sands off sectors I and II to expand south during only 3 years. This expansion took place not by an input of sands from elsewhere outside but by the redistribution of the sands pre-existent within the study area. The increase of gravel-containing areas over time attests to the formation of lag deposits via selective

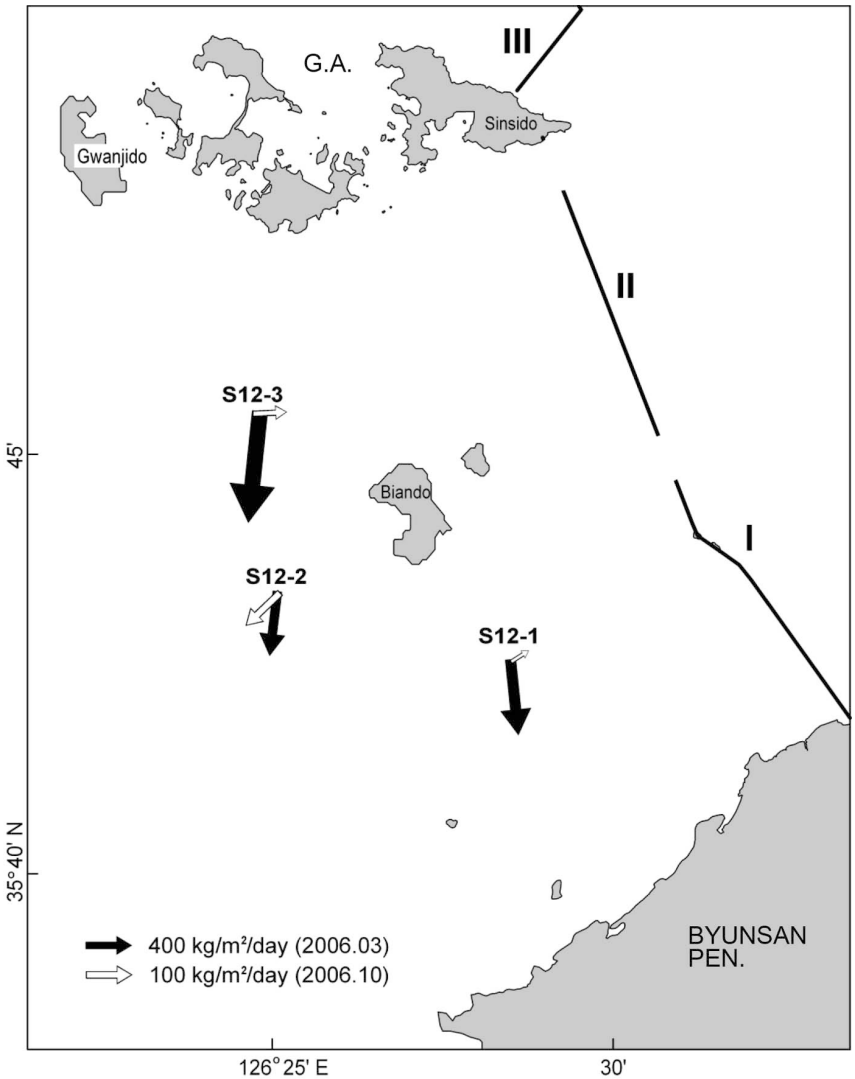

Fig. 14. Schematic of sediment transport vectors for two seasons (March and October) of 2006 in the study area. Note that the scales of vectors of the two seasons are much different from one another.

movements of sands. This phenomenon also implicitly supports that sands in the Saemangeum Area are mostly derived from the Mangyung and Dongin rivers which are now cut off from the outside of the dyke (KORDI, 2004). Off sector IV north of Gogunsan Archipelago, the surface sands are also found to have expanded widely in just 3 years 2002–2005 (Fig. 15) (Lee and Ryu, 2008). It is the northwesterly wind

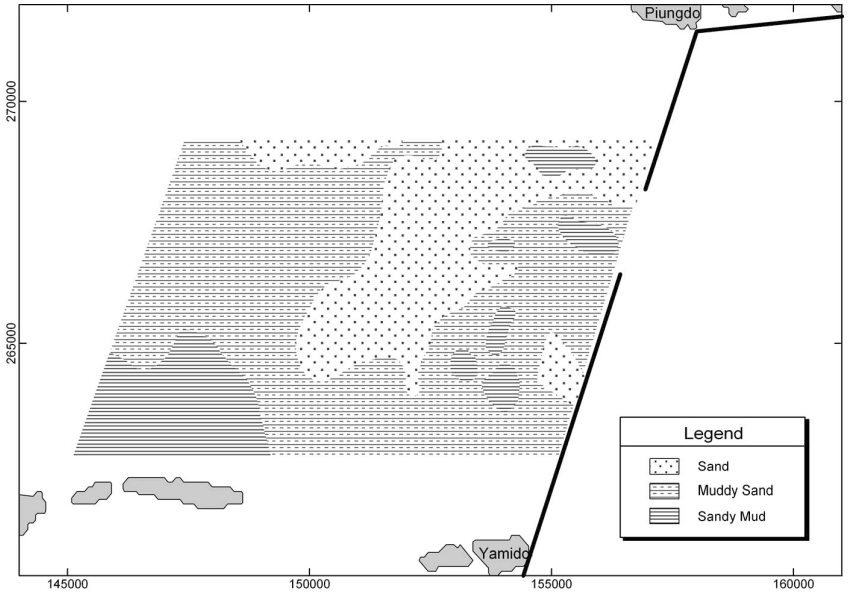

(a) 2002

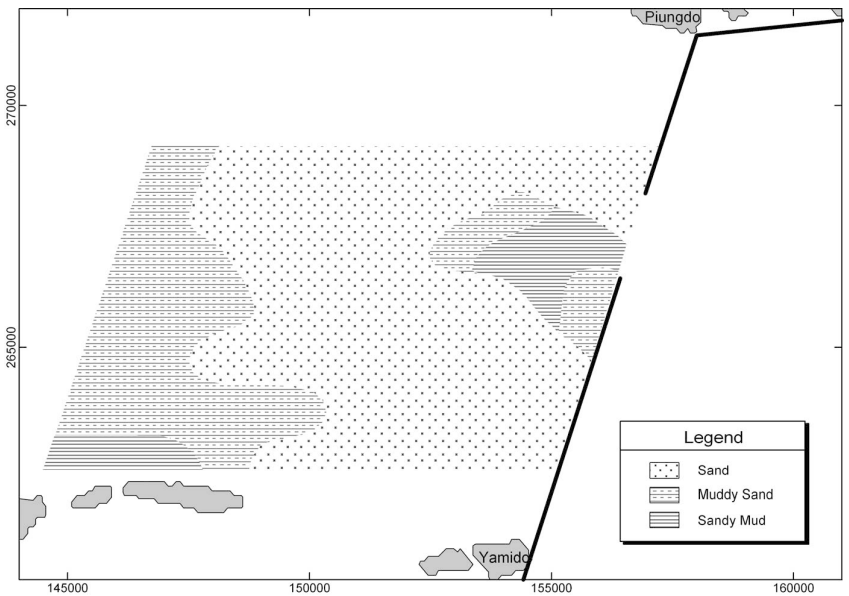

(b) 2005

Fig. 15. Distribution of surface sediments in (a) 2002 and (b) 2005.

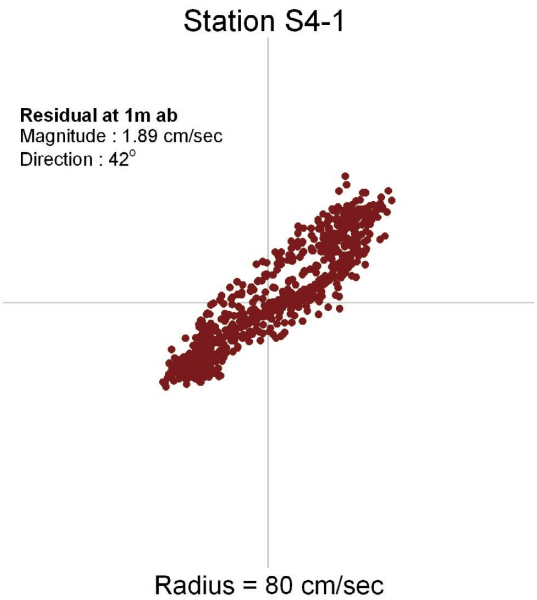

Fig. 16. Plot of current vectors from the 6-day records at station S4-1 off sector IV of the Saemangeum Dyke in May 2007.

in winter that accelerated southward movements of the sands, given that the rectilinear tidal currents here are intrinsically flood-dominant in the NE direction (Fig. 16). Hydrodynamic measurements with a TISDOS have revealed that residual currents began to flow south nearly concurrently with the NW winds resulting in the overturned tidal asymmetry with ebb dominance (Lee and Ryu, 2008). In general, the significant role of winter monsoon in transporting sands on the coastal area could explain why the offshore sands have accumulated onto the sand–mud mixtures on the shore (mostly tidal flats) during the mid-to-late Holocene resulting in the coarsening-upward coastal sequences in many places on the west coast of Korea (Fig. 17) (Chough et al., 2000).

Acknowledgments—This study is based on part of the results from a comprehensive project consecutively supported by the Ministry of Maritime Affairs and Fisheries since 2002, entitled 'Integrated Preservation Study on the Marine Environments in the Saemangeum Area' (grant no. PM54893).

REFERENCES

Chough, S.K., H.J. Lee and S.H. Yoon. 2000. *Marine Geology of Korean Seas*. Elsevier, New York.

Chough, S.K., H.J. Lee, S.S. Chun and Y.J. Shinn. 2004. Depositional processes of late Quaternary sediments in the Yellow Sea: a review, *Geosciences Journal* **8**: 211–264.

Clemens, S., P. Wang, W. Prell. 2003. Monsoons and global linkages on Milankovitch and sub Milankovitch time scales, *Marine Geology* **201**: 1–3.

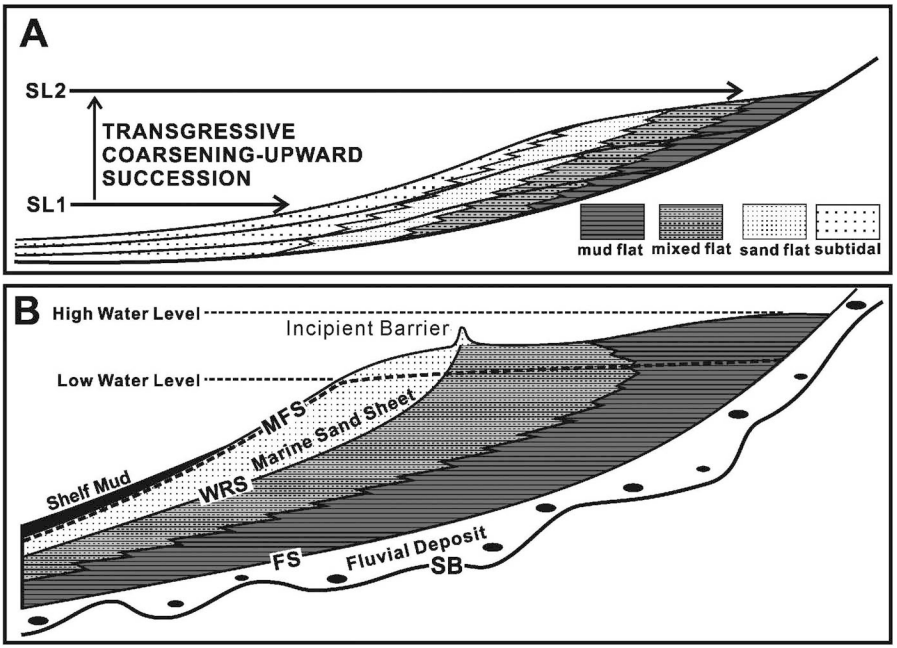

Fig. 17. Schematic diagram for evolutional history of Holocene tidal-flat deposits on Gomso Bay just south of the study area. Note two alternatives (A and B) suggested so far. After KORDI (2006).

KORDI. 1999. *A Pilot Study on Suspended Sediments Transport around the Saemankeum Dyke in Terms of Construction of Artificial Tidal Flats*. Report BSPE99772-00-1232-5, Korea Ocean Research & Development Institute (KORDI).

KORDI. 2004. *Integrated Preservation Study on the Marine Environments in the Saemangeum Area (2nd Year): Marine Geological Processes from Tidal Flats to Inner Shelf*. Report BSPM195-05-1581-5, Korea Ocean Research & Development Institute (KORDI).

KORDI. 2005. *Integrated Preservation Study on the Marine Environments in the Saemangeum Area (3rd Year): Projection and Management of Coastal Topographic Changes*. Report BSPM26008-1691-5, Korea Ocean Research & Development Institute (KORDI).

KORDI. 2006. *Integrated Preservation Study on the Marine Environments in the Saemangeum Area (1st Year of 2nd Phase): Projection and Management of Coastal Topographic Changes*. Report BSPM37907-1861-5, Korea Ocean Research & Development Institute (KORDI).

Lee, H.J. and S.K. Chough. 1989. Sediment distribution, dispersal and budget in the Yellow Sea. *Marine Geology* **87**: 195–205.

Lee, H.J. and Y.S. Chu. 2001. Origin of inner-shelf mud deposit in the southeastern Yellow Sea: Huksan Mud Belt. *Journal of Sedimentary Research* **71**: 144–154.

Lee, H.J. and S.O. Ryu. 2007. Role of the giant Saemangeum dyke in sedimentation at the mouth of an estuarine complex. *Marine Geology* **239**: 173–188.

Lee, H.J. and S.O. Ryu. 2008. Changes in topography and surface sediments by the Saemangeum dyke in an estuarine complex, west coast of Korea. *Continental Shelf Research* **28**: 1177–1189.

Lee, H.J., H.R. Jo, Y.S. Chu and K.S. Bahk. 2004. Sediment transport on macrotidal flats in Garolim Bay, west coast of Korea: significance of wind waves and asymmetry of tidal currents. *Continental Shelf Research* **24**: 821–832.

Lee, H.J., K.S. Bahk, H.R. Jo, Y.S. Chu, T.K. Kim, M.J. Kim, K.N. Kim and Y.G. Park. 2005. *Monitoring of Sedimentary Dynamical Behavior of Coastal Suspended Sediments*. Report BSPE90700-1728-5, Korea Ocean Research & Development Institute (KORDI).

National Oceanographic Research Institute. 2005. *Tide Tables (Coast of Korea)*. National Oceanographic Research Institute, Incheon, Korea.

National Oceanographic Research Institute. 2006. *Tide Tables (Coast of Korea)*. National Oceanographic Research Institute, Incheon, Korea.

Webster, P.J., V.O. Magana, T.N. Palmer, J. Shukla, R.A. Tomas, M. Yanai, T. Yasunari. 1998. Monsoons: processes, predictability, and the prospects for prediction. *Jounal of Geophysical Research* **103**: 14451–14510.

H. J. Lee (e-mail: heelee@kordi.re.kr)